# A Portable Intra-operative Framework applied to Distal Radius Fracture Surgery

Jessica Magaraggia[1,2,3], Wei Wei[2], Markus Weiten[2], Gerhard Kleinszig[2], Sven Vetter[4], Jochen Franke[4], Karl Barth[2], Elli Angelopoulou[1,3], Joachim Hornegger[1,3]

[1]Pattern Recognition Lab, FAU Erlangen-Nürnberg, Erlangen, Germany
[2]Siemens Healthcare GmbH, Erlangen, Germany
[3]Research Training Group 1773 "Heterogeneous Image Systems", Erlangen, Germany
[4]BG Trauma Center, Ludwigshafen am Rhein, Germany

**Abstract.** Fractures of the distal radius account for about 15% of all extremity fractures. To date, open reduction and internal plate fixation is the standard operative treatment. During the procedure, only fluoroscopic images are available for the planning of the screw placement and the monitoring of the instrument trajectory. Complications arising from malpositioned screws can lead to revision surgery. With the aim of improving screw placement accuracy, we present a prototype framework for fully intra-operative guidance that simplifies the planning transfer. Planning is performed directly intra-operatively and expressed in terms of screw configuration w.r.t the used implant plate. Subsequently, guidance is provided solely by a combination of locally positioned markers and a small camera placed on the surgical instrument that allows real-time position feedback. We evaluated our framework on 34 plastic bones and 3 healthy forearm cadaver specimens. In total, 146 screws were placed. On bone phantoms, we achieved an accuracy of $1.02 \pm 0.57$mm, $3.68 \pm 4.38°$ and $1.77 \pm 1.38°$ in the screw tip position and orientation (azimuth and elevation) respectively. On forearm specimens, we achieved a corresponding accuracy of $1.63 \pm 0.91$mm, $5.85 \pm 4.93°$ and $3.48 \pm 3.07°$. Our analysis shows that our framework has the potential for improving the accuracy of the screw placement compared to the state of the art.

## 1 Introduction

Fractures of the distal radius account for up to 15% of all extremity fractures. Open reduction and internal plate fixation is the most common operative treatment. During the procedure, intra-operative correct estimation of screw length and position under fluoroscopic control still represents a challenge. Among the reported complications (ranging from 6% to 80% [1]), several studies describe how the irregular anatomy of the distal radius leads to unrecognized cortical

The presented method is investigational use and is limited by law to investigational use. It is not commercially available and its future availability cannot be ensured.

perforation by screw tips, regardless of the art of locking plating: dorsal, palmar or volar [2,3]. Sugun et al. [2] reported a screw prominence rate of 25.65%, ranging from 0.5 to 6.1mm. In fact, depending on the type of view used (lateral, anterior-posterior, supinated, pronated, etc.) protrusions ranging from 3 to 6.5mm on average are required before protruding screws can be detected. It was also suggested that screw prominence greater than 1.5mm is likely to lead to complications [2]. Aurora et al. [3] reported that 9% of all complications are related to protruding screws, like plunging the drill bit into undesired soft-tissue structures and tendon rupture.Typically, revision surgery and implant removal are advised at the first sign of tendon irritation. Post-operatively, the severity of the complications associated with prominent screws is well recognized. An additional critical aspect is the intra-operative damage caused by perforation of the articulation compartments by the drill bit while preparing the insertion hole. In an extensive study conducted on cadaver forearms, Pichler et al. [4] reported a 43% incidence of drill bit violations of the third extensor compartment.

This leads to both a trial-and-error process during surgery for correct drilling and screw positioning, and to empty drill traces injuring soft tissue compartments [5]. Hence, practice advocates for solutions providing better intra-operative position control. Researchers continue investigating guidance techniques for orthopedic and trauma procedures. Although the usage of navigation solutions may increase the procedure time or involve some additional learning time, they successfully improve accuracy and reduce inter-user variability [6]. Commercial solutions like VectorVision (BrainLab) use an infrared stereo-camera and related markers. More recently, promising solutions for accurate screw placement have been proposed [7, 8], which, however require either a robotic arm or an augmented C-arm. Lately, Vetter et al. [9] presented the first clinical study on the use of an intra-operative planning application. However, in [9] plan transfer still strongly relied solely on the skills of the surgeon.

To support the surgeon in more accurate screw positioning, we developed a framework for combined intra-operative planning and guidance. For the planning, X-ray intra-operative images are acquired after fixing the plate onto the bone shaft. The plate model is then registered and an augmented view of the implant plate onto the acquired images supports the physician in deciding screw length and orientation. The core of our approach is the translation of the planning in a series of local plans for each screw. This allows the planning to be transferred under guidance support, which is provided solely by a combination of local markers fixed onto a conventional drill guide used for drilling (see Fig 1). Our augmented drill guide provides a local reference system onto the fixation plate. During the procedure, camera images are processed and correspondences are built between the detected marker-features and the real marker geometry. This allows the reconstruction of the position of the camera, and consequently of the attached instrument, in real-time w.r.t the plate, which was previously registered to the acquired X-ray images. Our method bypasses the need for bulky markers to be fixed onto the patient to provide a global patient reference as in conventional navigation systems [10]. Only small additional components such as

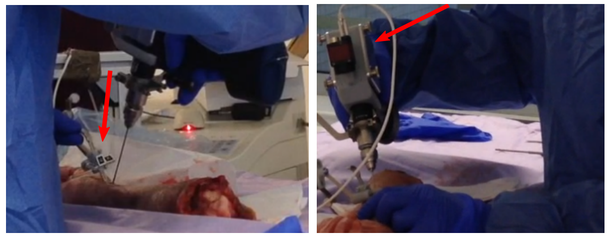

(a) (b)

**Fig. 1.** The hardware components of our design: (a) the drill guide with the attached markers and (b) the drill with the mounted camera.

markers and a video camera are required to be attached onto instrumentation already belonging to the standard clinical workflow. Our framework is general enough to adapt to several surgical fracture treatments, where precise screw positioning is required but bulky standard navigation systems are not applicable. In this study, the feasibility of our portable framework is shown. A prototype for reduction of distal radius fracture was built using standard surgical instrumentation. Extensive evaluation was performed on distal radius phantoms. First tests on forearm cadaver specimens were also carried out.

## 2 Methods

Our framework first allows the planning of the screw configuration required for fracture repositioning. Afterwards, the physician is supported during planning transfer via a flexible guidance solution that provides real-time position feedback of the drill. The current instrument position and its offset from the planned trajectory is visualized w.r.t the employed fixation plate and the patient anatomy.

### 2.1 Intra-operative Planning

Similarly to Vetter et al. [9] we also perform the planning intraoperatively. After fixing the plate onto the bone shaft, two X-ray images, a lateral, $\mathrm{I_{LAT}}$, and an anterior-posterior, $\mathrm{I_{AP}}$, are acquired using a mobile C-arm. An automatic 2D/3D registration is then performed to register the plate model, $\mathrm{P_L}$, to $\mathrm{I_{LAT}}$ and $\mathrm{I_{AP}}$. The registration result is described by the transformation matrices $\mathbf{T}_{\mathrm{LAT}}^{\mathrm{P_L}}$ and $\mathbf{T}_{\mathrm{AP}}^{\mathrm{P_L}}$. After registration, the plate model is overlaid to $\mathrm{I_{LAT}}$ and $\mathrm{I_{AP}}$. Using a comprehensive augmented overview of the complete plate-screw configuration, the physician determines the number of fixing screws, their orientation and length. The planning is then expressed as a set $\mathrm{X} = \{(\mathbf{P}_{\mathrm{T_i}}, \mathbf{v}_{\mathrm{A_i}})_{\mathrm{H_i}}\}$, where $(\mathbf{P}_{\mathrm{T_i}}, \mathbf{v}_{\mathrm{A_i}})_{\mathrm{H_i}}$ represent the screw tip position and the screw direction versor, respectively, in the local coordinate system of the i-th hole, $\mathrm{S_{H_i}}$, of the employed plate (see Fig. 2(a)). The transformation $\mathbf{T}_{\mathrm{P_L}}^{\mathrm{H_i}}$ is known by construction.

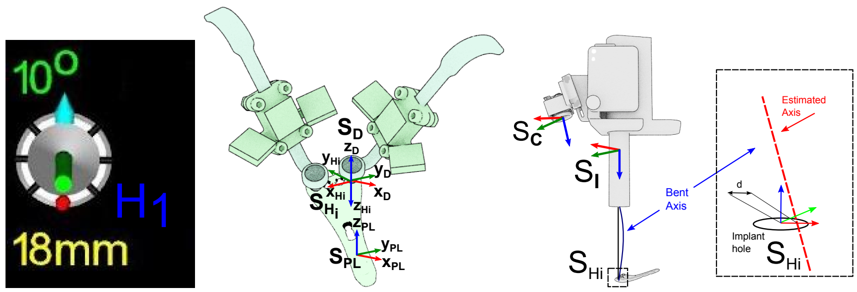


(a) (b) (c)

**Fig. 2.** (a) Local visualization of a screw plan. (b) A schematic representation of our augmented drill guide positioned on an implant plate. (c) Graphic depiction of the problem of the axis offset due to axis bending.

### 2.2 Intra-operative Guidance

The plate registration and parametrization of the planning in terms of the local set of coordinates X allow the guidance pipeline to be decoupled from a global patient reference. As we proposed in [11], we augment the drill guide, which is used for drilling support, with optical markers that can be seen from a small video camera mounted on a surgical drill. Holders for markers and camera were designed and then realized using rapid prototyping. They are mounted on standard surgical instrumentation (see Fig 1). The calibration of the camera-drill system, expressed by the transformation $\mathbf{T}_{\mathrm{C}}^{\mathrm{I}}$, allows us to express the position and orientation of the drill bit w.r.t the camera coordinate system $\mathrm{S}_{\mathrm{C}}$. Before drilling, the physician is asked to position the calibrated collection of drill guide-markers, $\mathrm{S}_{\mathrm{D}}$, onto the plate, as depicted in Fig. 2(b). Thus, $\mathrm{S}_{\mathrm{D}}$ does coincide with the local coordinate system of the current hole $\mathrm{S}_{\mathrm{H_i}}$.

While drilling, the markers placed onto the drill guide are inside the Field of View (FoV) of the camera. Marker detection and subsequent camera pose estimation, expressed by $\mathbf{T}_{\mathrm{D}}^{\mathrm{C}}$, are performed in real-time. Unlike our prior work [11], we employ binary encoded markers based on code redundancy similar to [12] and [13] in order to increase the robustness of marker identification especially w.r.t inhomogeneous illumination.

The geometric relations between plate hole, drill guide-markers, camera, and drill allow us to calculate the transformation $\mathbf{T}_{\mathrm{H_i}}^{\mathrm{I}}$, from $\mathrm{S}_{\mathrm{I}}$ to $\mathrm{S}_{\mathrm{H_i}}$, and hence the instrument position in real-time w.r.t $\mathrm{S}_{\mathrm{H_i}}$ as $(\mathbf{P}_{\mathrm{I}}, \mathbf{v}_{\mathrm{I}})_{\mathrm{H_i}}$. Depending on the selected drill guide position, a known transformation $\mathbf{T}_{\mathrm{D}}^{\mathrm{H_i}}$ exists between the two coordinate systems $\mathrm{S}_{\mathrm{H_i}}$ and $\mathrm{S}_{\mathrm{D}}$ (see Eq. 1). In our previous work [11], we showed that the accuracy of the estimated position is affected by the vibration of the instrument, that negatively impacts the image quality. A reported cause was the instrument contact with the surrounding components in particular during the perforation of the bone surface. By quantifying the image blur at the edges of the markers we can exclude highly blurred images from our computations. Moreover, the user is advised to follow the natural sequence of 2 steps: 1) Targeting and 2) Drilling. Thus, motion blur is minimized during targeting.

$$\mathbf{T}^{\mathrm{I}}_{\mathrm{H_i}} = \mathbf{T}^{\mathrm{D}}_{\mathrm{H_i}} \mathbf{T}^{\mathrm{C}}_{\mathrm{D}} \mathbf{T}^{\mathrm{I}}_{\mathrm{C}} \tag{1}$$

$$\mathbf{T}^{\mathrm{I}}_{\mathrm{AP}} = \mathbf{T}^{\mathrm{P_L}}_{\mathrm{AP}} \mathbf{T}^{\mathrm{H_i}}_{\mathrm{P_L}} \mathbf{T}^{\mathrm{I}}_{\mathrm{H_i}} \tag{2}$$

The previously performed 2D/3D registration between the plate model and the intra-operative X-rays allows us to report the instrument position directly onto $\mathrm{I_{AP}}$ (see the final transformation, $\mathbf{T}^{\mathrm{I}}_{\mathrm{AP}}$, in Eq. 2). The same can be done for $\mathrm{I_{LAT}}$. Hence, our guidance design reports the instrument position w.r.t the patient anatomy without the need for additional marker reference to be fixed onto the patient, as traditional navigation systems would require.

### 2.3 Instrument Visualization

Visualization of the instrument position is performed 1) on a simplified but comprehensive scene focusing on the local visualization w.r.t the drill guide $\mathrm{S_D}$ and 2) as a 3D overlay onto $\mathrm{I_{LAT}}$ and $\mathrm{I_{AP}}$. As with all hand-held instruments, depending on the diameter and length of the drill bit, bending of the drill axis can occur during the operation. However, our instrument calibration is expressed by the rigid transformation $\mathbf{T}^{\mathrm{I}}_{\mathrm{C}}$. A bending of the axis undermines our rigidity assumption (see Fig. 2(c)). Although no modeling for the axis bending can be applied, safety concerns require the recognition of these critical cases. Recall that the drill bit trajectory is constrained to pass through the origin $\mathrm{O_{H_i}}$ of $\mathrm{S_{H_i}}$. The intersection $\mathrm{P_{A_i}}$ between the estimated axis trajectory and the plane orthogonal to hole axis is calculated. Values of the distance $d = \overline{\mathrm{O_{H_i}}, \mathrm{P_{A_i}}} \neq 0$ are considered as an indication of the axis bending. A warning is given to the user, suggesting that attention should be paid while holding the instrument.

## 3 Experiments

Extensive experiments were conducted both on distal radius bone phantoms and on healthy forearm cadaver specimens. A total of 34 (15 rights and 19 left) phantoms (involving 135 screws) and 3 specimens (2 rights and 1 left involving 11 screws for which the drill guide was correctly oriented) were used in our evaluation. The length of the screws ranged from 14 to 24mm. Two user groups (4 users with engineering expertise and 2 medical experts) operated on the phantoms. The specimens were operated by just one medical expert. According to the proposed workflow, for each test, the operator was asked to: 1) fix the implant to the test-body, 2) acquire 2 radio-graphic images for implant registration, 3) plan the desired screw configuration, 4) select the current screw hole and accordingly position our marker-drill guide, 5) transfer the plan guided by the real-time feedback of our software, and 6) place the screws and acquire a 3D volume (Arcadis® Orbic 3D, Siemens; Volume: $256^3$ voxels; Spacing: 0.485mm). After manual registration of the plate to the 3D volume, we evaluated the accuracy

**Table 1.** Mean and median values for tip distance ($d_T$), and for errors in azimuth ($\alpha$), elevation ($\beta$) and total ($\psi$) angles for plastic bones: 1) All users (AU), 15 right bones (60 screws) and 19 left bones (75 screws); 2) Engineering experts (EE), 13 right bones (52 screws) and 17 left bones (67 screws); 3) Medical experts, (ME) 2 right bones (8 screws) and 2 left bones (8 screws). The last row refers to the forearm specimens (FS).

| | $d_T$ (mm) | | $\alpha$ (°) | | $\beta$ (°) | | $\psi$ (°) | |
|---|---|---|---|---|---|---|---|---|
| AU | $1.02 \pm 0.57$ | 0.89 | $3.68 \pm 4.38$ | 2.60 | $1.77 \pm 1.38$ | 1.49 | $2.52 \pm 1.62$ | 2.18 |
| EE | $0.97 \pm 0.47$ | 0.89 | $3.29 \pm 4.02$ | 2.45 | $1.76 \pm 1.34$ | 1.52 | $2.43 \pm 1.37$ | 2.18 |
| ME | $1.34 \pm 1.02$ | 1.06 | $5.86 \pm 6.18$ | 3.18 | $1.85 \pm 1.73$ | 1.21 | $3.21 \pm 2.87$ | 2.39 |
| FS | $1.63 \pm 0.91$ | 1.40 | $5.85 \pm 4.93$ | 4.07 | $3.48 \pm 3.07$ | 2.17 | $4.54 \pm 2.77$ | 4.37 |

of the transferred plan in terms of the Euclidean distance of the screw tip, $d_T$, and of the absolute errors in the screw axis orientation, expressed in azimuth, $\alpha$, elevation, $\beta$, as well as total, $\psi$, angles (see Table 1). Our error estimates contain all 6 process steps. Our ANOVA analysis showed significant ($p < 0.05$) difference in $d_T$ and no significant difference ($p > 0.05$) in $\psi$ between EE and ME.

## 4 Discussion and Conclusions

Our portable framework for intra-operative planning and guidance for distal radius fracture surgery does not require the fixation of any navigation markers onto the patient. The patient reference is provided directly by the plate registration onto the images acquired intra-operatively. For guidance, minimal additional instrumentation is required. The feasibility of our framework and its impact on screw positioning accuracy were investigated. For performance comparison, we recall the closest related work [9], a clinical study conducted using solely intra-operative planning. Though their results refer to real cases, we can still use them as a point of reference for the expected accuracy without a guidance system: their reported errors in $d_T$, $\alpha$ and $\beta$ are 2.24±0.97mm, 18.69±29.84° and 1.66±4.46° respectively. The series of our evaluations conducted in a lab environment on phantoms (see Table 1), showed overall a significant increase in screw placement accuracy and robustness. The mean error in $d_T$ and $\alpha$ was reduced by 54% and 80% respectively, while the standard deviation dropped by 41% and 85% accordingly. The mean error in $\beta$ increased from 1.66° to 1.77°, while the standard deviation was more than halved. As expected, the error distribution (see Fig. 3) shows that higher error occurs when drilling in the north sector, i.e. close to the marker holder, since this reduces marker visibility. In these specific cases, appropriate drill guide rotation is expected to increase accuracy.

A similar performance was observed in the experiments conducted on forearm specimens. The mean error in $d_T$ and $\alpha$ was reduced by 27% and 69% respectively, while the standard deviation was decreased by 6% and 83% accordingly. The mean error in $\beta$ increased from 1.66° to 3.48°, while the standard deviation was decreased by 31%. In one of the right forearms, the drill guide for one of the

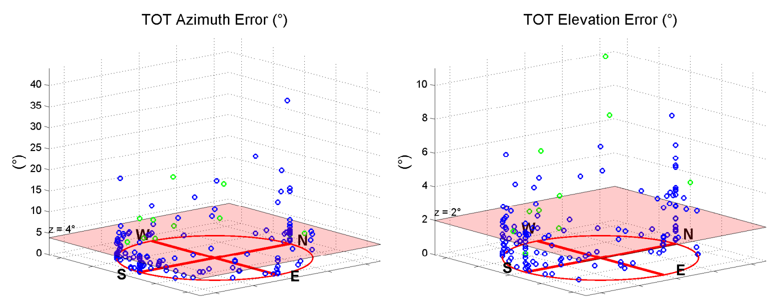


(a) (b)

**Fig. 3.** Error distribution for the 4 angular sectors for phantoms (blue) and specimens (green): (a) azimuth and (b) elevation. North relates to the distal side of the plate.

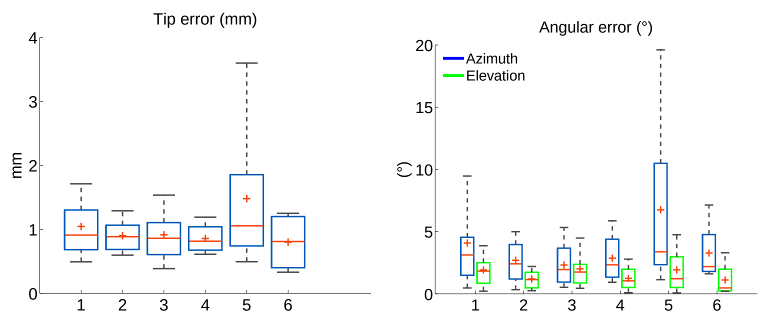


(a) (b)

**Fig. 4.** Inter-user variability for the bone phantoms in terms of (a) the tip error, and (b) the angular error in azimuth and elevation. Users 1 to 4 are engineering experts, while 5 and 6 are medical experts. Users 4 and 6 operated each on a single phantom.

screws was rotated 90° w.r.t the planned position. Although our software allows selecting the drill guide orientation for planning transfer, in this case the change in orientation was not conveyed by the user. Even under such circumstances, our guidance framework helped keep mean error values for both $\alpha$ and $\beta$ below 10° and 4° respectively. Introducing the above mentioned case of incorrectly positioned drill guide into our quantitative evaluation, results in errors in $d_T$, $\alpha$ and $\beta$ of 1.94±1.37mm, 9.00±11.89° and 3.32±2.98° respectively. Moreover, our sequential analysis showed that the performance of user 5 improved over time for both phantoms and forearm specimens. A fourth specimen was excluded from the quantitative evaluation, since plate rotation occurred during the procedure. Our results show that our framework is expected to increase the accuracy in screw positioning and to improve robustness. Further testing is to be performed on specimens presenting common fracture types.

## Acknowledgements

This work was supported by the Research Training Group 1773 "Heterogeneous Image Systems", funded by the German Research Foundation (DFG).

## References

1. McKay, S.D., MacDermid, J.C., Roth, J.H., Richards, R.S.: Assessment of complications of distal radius fractures and development of a complication checklist. Journal of Hand Surgery **26**(5) (2001) 916–922
2. Sügün, T., Karabay, N., Gürbüz, Y., Özaksar, K., Toros, T., Kayalar, M.: Screw prominences related to palmar locking plating of distal radius. Journal of Hand Surgery (European Volume) **36**(4) (2011) 320–324
3. Arora, R., Lutz, M., Hennerbichler, A., Krappinger, D., Espen, D., Gabl, M.: Complications following internal fixation of unstable distal radius fracture with a palmar locking-plate. Journal of Orthopaedic Trauma **21**(5) (2007) 316–322
4. Pichler, W., Grechenig, W., Clement, H., Windisch, G., Tesch, N.: Perforation of the third extensor compartment by the drill bit during palmar plating of the distal radius. Journal of Hand Surgery (European Volume) **34**(3) (2009) 333–335
5. Al-Rashid, M., Theivendran, K., Craigen, M.: Delayed ruptures of the extensor tendon secondary to the use of volar locking compression plates for distal radial fractures. Journal of Bone & Joint Surgery, British Volume **88**(12) (2006) 1610–1612
6. Jenny, J.Y., Miehlke, R.K., Giurea, A.: Learning curve in navigated total knee replacement. a multi-centre study comparing experienced and beginner centres. The Knee **15**(2) (2008) 80–84
7. Koutenaei, B.A., Guler, O., Wilson, E., Thoranaghatte, R.U., Oetgen, M., Navab, N., Cleary, K.: Improved screw placement for slipped capital femoral epiphysis (SCFE) using robotically-assisted drill guidance. In Golland, P., Hata, N., Barillot, C., Hornegger, J., Howe, R., eds.: MICCAI 2014, Part I. Volume 8673 of LNCS. Springer International Publishing (2014) 488–495
8. Diotte, B., Fallavollita, P., Wang, L., Weidert, S., Thaller, P.H., Euler, E., Navab, N.: Radiation-free drill guidance in interlocking of intramedullary nails. In Ayache, N., Delingette, H., Golland, P., Mori, K., eds.: MICCAI 2012, Part I. Volume 7510 of LNCS. Springer Berlin / Heidelberg (2012) 18–25
9. Vetter, S., Mühlhäuser, I., von Recum, J., Grützner, P.A., Franke, J.: Validation of a virtual implant planning system (VIPS) in distal radius fractures. Bone & Joint Journal Orthopaedic Proceedings Supplement **96**(SUPP 16) (2014) 50–50
10. Frank, J., Gritzbach, B., Winter, C., Maier, B., Marzi, I.: Computer-assisted femur fracture reduction. European Journal of Trauma and Emergency Surgery **36**(2) (2010) 151–156
11. Magaraggia, J., Kleinszig, G., Wei, W., Weiten, M., Graumann, R., Angelopoulou, E., Hornegger, J.: On the accuracy of a video-based drill-guidance solution for orthopedic and trauma surgery: preliminary results. In: SPIE Medical Imaging, International Society for Optics and Photonics (2014) 903610–903610
12. Wagner, D., Schmalstieg, D.: Artoolkitplus for pose tracking on mobile devices. In: CVWW'07, 12th Computer Vision Winter Workshop, Sankt Lambrecht, Austria. (2007)
13. Fiala, M.: Artag fiducial marker system applied to vision based spacecraft docking. In: IROS, Workshop on Robot Vision for Space Applications. (2005) 35–40